Hybrid Energy Systems: The Demand Side

Elizabeth Buechler[1], Chris Juchau[2], Sandra Cardon[3] and John Gardner[3]

Nomenclature

Symbol/Abbreviation	Unit	Definition
C_b	kWh	Battery capacity
C_{pv}	kW	PV capacity
D	h	Peak load duration; hours per day that the load is greater than 90% of the daily peak load
E_a	kWh	Annual energy purchased from a utility not factoring in any excess PV energy sold back through a net metering agreement
E_{90}	kWh	Area under a load duration curve above the 90th%ile of the original load
$E_{90,avoid}$	kWh	E_{90} avoided; the difference between E_{90} of an original and modified load
GPL	kW	Grid power limit; measured in terms of a percentile on a monthly net PV load duration curve
N_h	---	Number of houses in a microgrid; N_h=1 for a single house
P	kW	Electrical load at time t
P_p	kW	Annual peak load; maximum point on a load duration curve
$P_{p,red}$	kW or %	Reduction in P_P
P_{pv}	kW	PV power at time t
P_s	kW	Battery power at time t; positive = charging, negative = discharging
P_{90}	kW	90th percentile on a load duration curve; the level of power the load is below 90% of the year
$P_{90,red}$	kW or %	Reduction in P_{90}
Q_b	kWh	Battery charge at time t
RC_b, RD_b, RC_C, RD_C, RC_S, RD_S	kW	Maximum charging (RC) and discharging (RD) rates for the battery (b), controller (c), and entire storage system (s)
η_b	%	Roundtrip battery storage efficiency

Introduction

The rapid expansion of renewable electric generation based on wind and solar resources has brought with it significant technical challenges due to its variable and somewhat unpredictable nature. The

[1] College of Engineering, Tufts University
[2] CAES Energy Policy Institute, Boise State University
[3] CAES Energy Efficiency Research Institute, Boise State University

judicious combination of various generating technologies, leveraging the various strengths to overcome these challenges has brought about renewed interest in so-called Hybrid Energy Systems. These analyses broaden the energy problem by considering non-electrical energy flows. For example, the thermal energy from a nuclear power plant can be rapidly diverted from a traditional steam generator to an industrial process that requires significant heat such as biofuel production{reference Humberto's papers here}. This paper makes the case that, whereas these approaches show considerable promise, this approach can be even more powerful if combined with innovative system combinations on the demand side as well. We present a framework for the implementation, control and modeling of a micro-grid with distributed generation, local storage and demand response as shared and holistic resources. Our focus was on peak reduction and load shifting, as opposed to simple kWh production, which is typical of residential systems.

Methodology

We used standard DOE energy modeling tools to develop a baseline residential energy load. A "typical" residential structure for SW Idaho was created in BeOpt, then modeled in Energy+, using the TMY3 file for Boise, Idaho as the input. PV generation was also modeled within Energy+ and the results for a 1kW array was used as the base for scaling. The output of the Energy+ modeling was then imported to the Matlab environment where various PV capacities and number of homes could be combined. Matlab was also used to develop an optimized energy storage strategy. Finally, published electric utility tariffs and historic spot prices were used to develop an economic model in an attempt to find the value both distributed generation and storage provide to the homeowner and the utility. Details of the methodology follow.

1. Residential Building Model

Electrical load and PV production data with a 15-minute time step was generated with the simulation engine EnergyPlus. The NREL program BEopt, which serves as an interface between the user and EnergyPlus was used to generate an EnergyPlus input file. The input file needed to be modified before simulation because of various modeling limitations in the BEopt program. The 2011 Residential Building Stock Assessment from the Northwest Energy Efficiency Alliance [2] and the 2009 Residential Energy Consumption Survey (RECS) from the U.S. Energy Information Administration [3] were used as references to determine the characteristics of a typical home in the Boise, Idaho region. The Residential Building Stock Assessment outlines building characteristics and energy use patterns specific to the northwestern US and Idaho. The RECS document has a more general approach, and discusses the aggregate characteristics of Idaho, Montana, Utah and Wyoming as well as the western US as a whole. All remaining building design characteristics that were necessary for the simulation were determined according to the NREL New Construction B10 Benchmarks [4] which vary with each IECC zone. A TMY3 Boise Air Terminal weather file was also used as input for the simulation in order to account for local weather trends.

Table 1: Housing characteristics of the modeled Boise, ID house

Finished space	2188 sq. ft.
Room characteristics	4 bedrooms, 3 bathrooms, crawlspace, unfinished attic
Wall Insulation	R-13 Fiberglass Batt
Cooling system	Central air conditioning SEER 13
Heating system	Gas furnace
Windows	311 total sq. ft., double pane
Appliances	Refrigerator, electric cooking range, dishwasher, clothes washer, clothes dryer
Benchmark appliances*	Extra refrigerator, freezer, pool heater and pump, hot tub heater and pump, well pump, gas fireplace, gas grill, gas lighting
*Benchmark appliances are accounted for as a fraction of a whole appliance (typically very small), depending the likelihood that a home would actually own and use the appliance.	

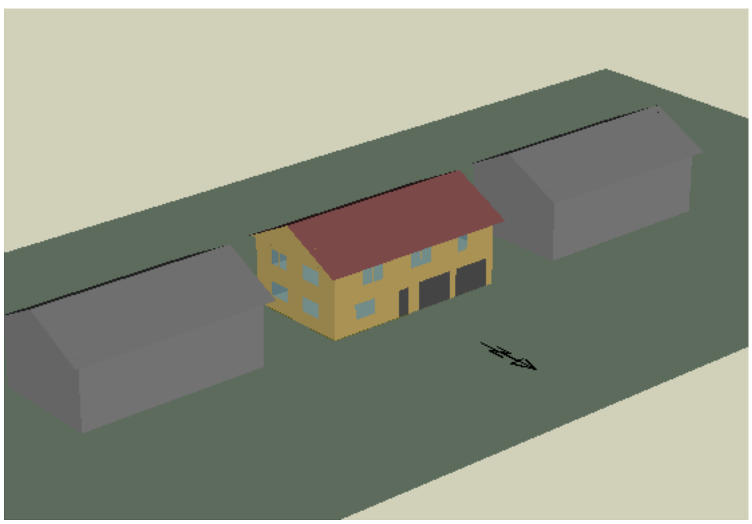

Figure 1: Rendering of prototypical SW Idaho home used in study

2. PV array generation

The PV function scales annual PV production data from EnergyPlus for a 1kW west facing array to the specified capacity. The assumption was made that PV production increases proportionally with PV capacity in relation to a 1 kW array.

$$P_{pv,CkW} = P_{pv,1kW} * C_{pv}$$

A linear regression model to model DR is currently being prepared. This study has so far only produced results for the implementation of PV and storage, but future work will hopefully be done to investigate the effects of applying all three technologies.

3. A Residential Microgrid

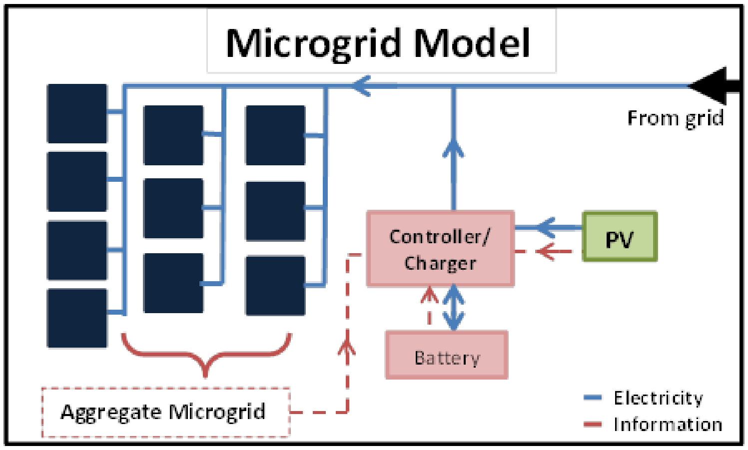

Figure 2: Conceptual Model of the Residential Microgrid

Figure2 1 is the schematic representation of the residential microgrid envisioned in this study. Note that the PV, battery and controller, while likely to be installed in one or more of the grid's residences, they are not considered owned by individual homeowners. Likewise, the economic and energy benefits from the additions will not be considered applicable to any one resident. This distinction will be made clearer in the 'economic modeling' section.

4. Storage optimization

Since battery storage is normally used for off-grid applications rather than system benefit, many of the storage algorithms that are discussed in literature are not optimal for this study. For a house to go completely off-grid, the load must be met entirely with PV power and discharge from storage. A storage algorithm for that purpose might adhere to the following logic:

$$if\ P > P_{pv}\ then\ P_s = -(P - P_{pv})$$
$$if\ P < P_{pv} then\ P_s = P_{pv} - P$$

(Assuming the constraints C_b, RC_s, and RD_s are obeyed)

The battery would be discharged when there was a power deficit, and it would be charged when there was excess power, without violating the battery constraints. On the other hand, our vision for a microgrid is a system with a relatively small amount of PV and storage capacity compared to the size of the aggregate microgrid load, making it unrealistic to go off-grid. Instead, the overall system benefits by reducing both peak load and amount of energy consumed during peak periods through optimization of the entire system within the microgrod.

The logic flow chart for the storage algorithm that was used in this study has been included in the appendix. It depends on the relative values of P, P_{pv}, Q_b, and the grid power limit (GPL). The GPL is an input value for the algorithm, and it is the maximum level of power the grid must supply. It must be set at an optimal level so that the battery does not run out of charge during a peak load. An example of the resulting load profile after PV and storage have been applied to a single house is shown in Figure 3. The peak loads flatten out at a level of power equal to the GPL. The implication of this type of storage system is that a utility company can be confident that a load will not exceed the GPL as long as the GPL has been set at an appropriate level.

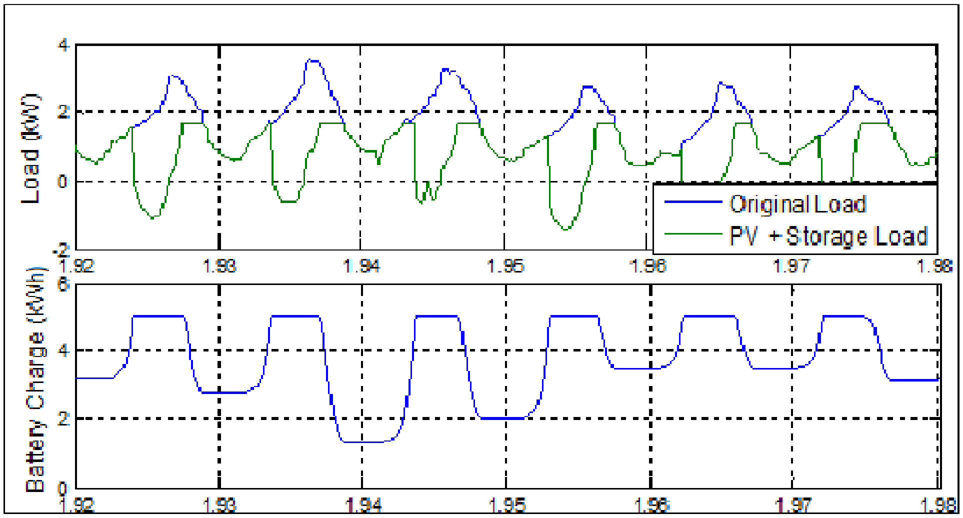

Figure 3: Load profile and battery charge of a single house with a PV + storage system (5kw PV, 5kwh battery storage)

J. Leadbetter and L. Swan (2012) studied peak load shaving with the application of an inverter/charger and battery storage where the grid was used as an energy source instead of PV [5]. The Leadbetter storage algorithm is similar to the one used in this study, in that both of them use a grid demand limit [5]. The Leadbetter grid demand limit was set to a constant value equal to a certain percentile on the load duration curve [5]. The GPL in our model varies throughout the year to account for fluctuations in the load of a typical Boise house. A GPL that varies from month to month is more practical to implement than a daily GPL, and is more effective in reducing peak loads than a yearly one.

The optimal GPL is simple to calculate after the fact with actual load and PV data, but much more difficult ahead of time with limited information. In order to associate it with a variable that can be observed or predicted, the GPL was linked to a certain percentile on the monthly net PV load duration curve. A homeowner could make calculations from load and PV data from previous years. One of the purposes of this study is to determine what range of GPL percentiles results in efficient energy storage.

A simulated annealing solving algorithm was used to determine the optimal GPL that minimizes some output variable (P_P, E_{90}, etc.). Results from multiple iterations of the exact same simulation vary slightly because a random number generator is a component of the solving algorithm [6]. The optimizations were performed for a range of values of the input variables C_{PV}, C_B and N_H.

5. Economic modeling

The analysis presented in this section seeks to estimate the potential value of a neighborhood microgrid from the perspectives of an investor owned utility (IOU) and a group of homeowners served by the IOU. Placing small generation systems inside of electric distribution networks is not a new idea and proponents and detractors often differ in their assessment of the actual costs and benefits of adding distributed generation to electricity grids (Daley and Morrison, 2001).

The economic analysis presented in this paper is based on an assumed aggregation of 10 houses in a neighborhood in the Boise, ID area each with electrical loads as described earlier in the paper. The group of ten homes is modeled with increasing shared PV generation and electricity storage capacities. It was assumed that the 10 house microgrid does not supply power or service back to the grid, but rather uses its DG and storage resources primarily to reduce peak demand and secondarily to reduce energy consumption. The value of each system was estimated based on prevailing utility rates schedules to approximate potential customer savings. The avoided cost of each system as viewed by the utility was then estimated using published avoided cost rates. The load profiles for four different scenarios were analyzed over a one year time period at 15 minute intervals. The four scenarios modeled for analysis are as follows:

1) Baseline scenario: no distributed generation or storage
2) 5 x 5 scenario: Five kW of PV combined with five kWh of battery storage
3) 10 x 10 scenario: Ten kW of PV combined with ten kWh of battery storage
4) 20 x 20 scenario: Twenty kW of PV combined with twenty kWh of battery storage

The rate structures used to estimate the avoided cost of purchased power from the homeowner's perspective are based on Idaho Power's current published rate schedules (Idaho Power, 2014). Idaho Power's rates were chosen simply because the weather files and housing models used are specific to the Boise, Id area and Idaho Power is the IOU that provides electrical service to Boise consumers. Two different rate schedules were selected in order to compare two different, and fairly common, methods utilities use to calculate customer charges. The first rate structure selected was the standard residential rate plan which consists of three volumetric pricing tiers under which residential customers pay more per kWh with increasing electricity consumption per each billing period. Such a rate plan seeks recovery for both fixed and variable utility costs almost entirely through energy charges and is designed to encourage conservation (Blank and Gegax, 2014).

The second rate plan selected was the Large General Services (LGS) rate. The LGS rate was selected because it is an example of a straight-fixed-variable (SFV) rate that incorporates both fixed demand charges and variable energy charges to recover utility service costs (Blank and Gegax, 2014). The LGS plan also incorporates energy charges that vary by time of day and season in contrast to standard residential rates which only vary by season and volume of use. SFV plans incentivize a customer to increase their load factor by decreasing peak demand, increasing average energy use, or using some combination of those two approaches. A net metering schedule was not evaluated due to the assumption that the ten house microgrid only provides behind the meter service and does not feed power or services back to the grid. The standby rate schedule has been avoided for the moment due to the need to make assumptions about contracted supply and the large minimum demand and energy requirements thresholds dictated by the rate schedule.

6. Indices of performance

In addition to the economic models, we also focused on engineering variables that indicate characteristics most likely to be beneficial to overall system operation. Figure 4 shows the primary indices of performance on a load duration curve.

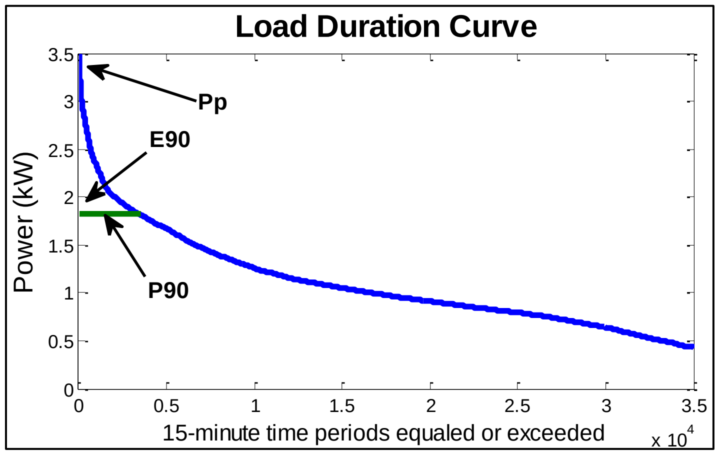

Figure 4: Load duration curve of prototypical home load

Peak Power, Pp: The load duration curve (a plot of demand level ordered by total amount of time experienced at that level shows the peak annual power (on 15 minute basis). This is the number often used by utilities to set the Basic Load Capacity charge (or ratcheting demand charge). Utilities have to maintain the distribution system to accommodate this power level, even if it happens only once in the course of a year. Reducing this level throughout the system makes the system more robust to technical issues and more able to accommodate load growth.

90^{th} percentile Power, P90: Similar to the peak power, this power is the level below which the demand is 90 % of the year. The difference between Pp and P90 is indicative of how 'peaky' the load is.

90^{th} percentile Energy, E90: This is the amount of energy (in kWh) consumed above th eP90 level. Arguably, this is consistently the most expensive energy for the utility to deliver and sometimes comes from the spot market at the same time the spot market prices are peaking. Reducing E90 energy consumption can reduce overall costs to the utility and the ratepayer.

Results To Date

1. South vs West PV panels

The science of solar energy harvesting clearly indicates that maximum power conversion for fixed (non tracking) panels occurs when the panels are oriented southward (in the northern hemisphere) and tilted from the horizontal at an angle equal to the latitude of the installation. If however you relax the requirement of maximum kWh yield and focus on other benefits (such as reduced peak) different orientations are beneficial. Figure 5 shows the indices of performance for a single prototypical home with PV installation for south facing vs west facing PV arrays. In both cases the arrays were roof mounted on a x by x roof pitch (xx degress vs 43.6 deg latitude)

Note that south facing panels reduce the peak by approximate 8% while the westfacing arrays reduce peak by more that 12%. Also of note, maximum peak redciton occurs with a relative small array (less than 2 kW). The P90 and E90 plots show similar results, indicating that west facing arrays perofrm better and the spread relative to south facing arrays is greatest where the relative benefit is greatest (the 'knee' of the curves). Finally, we note that the amount of energy purchased making up an deficit between generation and consumption, is nearly the same for both array orientations. In general the south facing array will produce 25% more energy than west facing arrays under standard conditions.

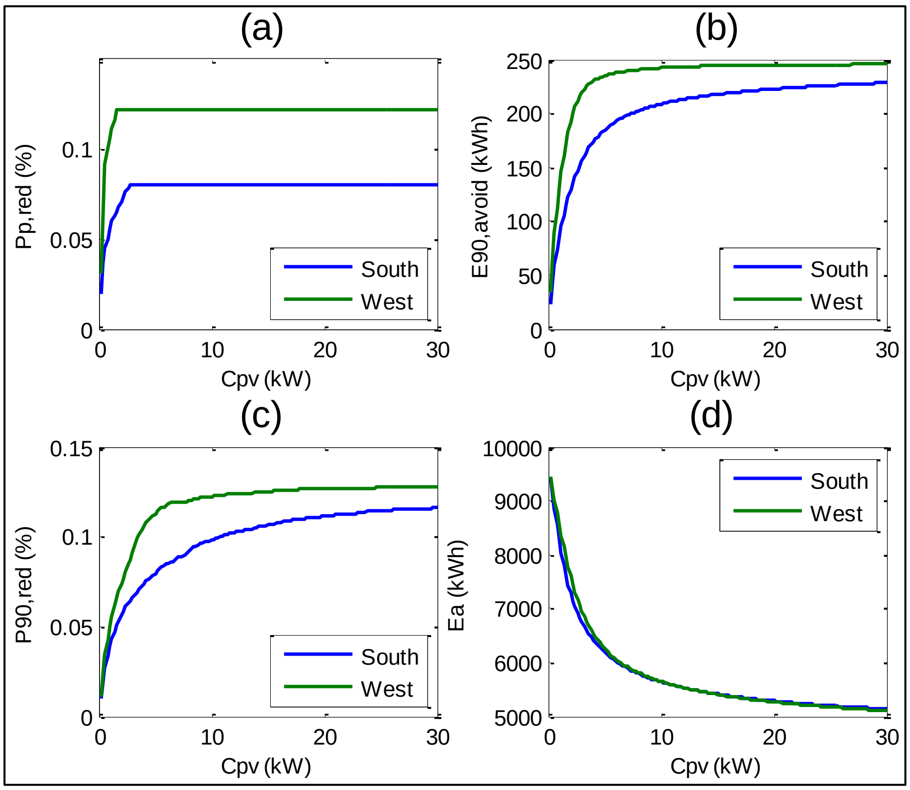

Figure 5: Impact of PV panel orientation on indices of performance.

All three indices of performance (Pp, P90 and E90) show similar characteristics in that the point of diminishing returns for higher PV capacity occurs at relatively low values. For example, the home simulated would reach net-zero with south facing panels at a capacity of about 6 kW, yet west facing panels near maximum benefit at 2 to 2.5 kW.

This feature led us to believe that a typical installation of 5-10 kW would generate system benefit that could be interpreted as being shared by the immediate neighbors. In this sense, we define a neighbor in the sense of the distribution system: those homes on the same distribution feeder as the home with the PV array.

Figure 6 shows the reduction in peak power if the PV capacity is used to reduce peak power in a number of homes. The lowest line (in blue) shows the same result indicated in figure 5(a). The plot indicates that a single 5 kW array (or accumulated 5 kW capacity over several homes), west facing at roof pitch, will reduce the peak load of one home by about ½ kW, but if spread over the aggregated load of 7 homes, the benefit of that same PV capacity is 5 times greater, reducing the aggregate peak load of 7 homes by a total of 2.5 kW. Maximum peak reduction for a group of 10 homes occurs with about 16 kW of capacity and an overall reduction of 4.4 kW.

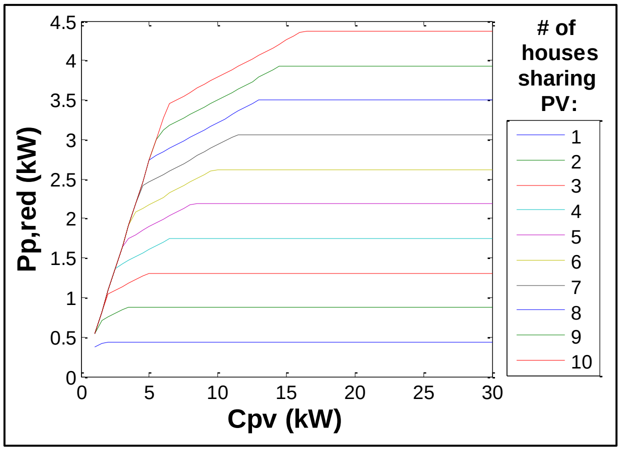

Figure 6: $P_{p,red}$ as a function of C_{pv} for different numbers of houses sharing PV

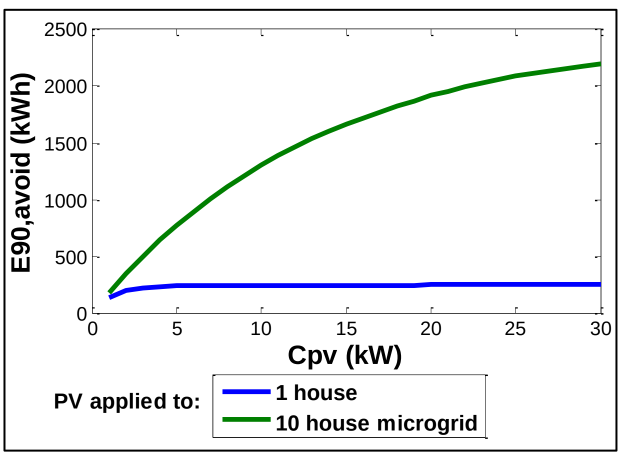

Figure 7: $E_{90,avoid}$ as a function of C_{pv} for a single house and a 10 house microgrid collectively using PV

PV can only reduce the peak load of a single home to a certain limit, which is equal to the maximum load when there is no PV power. As discussed previously, a small amount of west facing PV capacity is needed to reduce the peak load to this limit (approximately 1.8 kW), and any additional capacity has no effect. A home with more than approximately 1.8 kW west-facing PV capacity could share PV power with a second home and reduce the peak load of the second home without necessarily affecting the first. Figure 6 shows that as the number of homes sharing PV increases, the limit of P_{PRed}

increases proportionally. The maximum $P_{p,red}$ (kW) is 0.44 kW for a single house and 4.37 kW for a 10 house microgrid.

The specific bends in the curves in Figure 6 are explained by the shift in the peak load as C_{pv} increases. The slope is equal to P_{pv} at the time of the peak. Originally the peak occurred at 5:00 PM on July 21, when P_{pv} was high. With a certain increase in C_{pv}, the peak PV net load shifted to 7:15 PM when P_{pv} was not as high. The curve flattened out because P_{pv} =0 at the time of the peak when the peak shifted even later. The bent nature of the curve may partially be due to the 15-minute time step of the data.

For a single house, $E_{90,avoid}$ increases asymptotically to a certain limit as C_{pv} increases. As Figure 7 shows, the asymptote increases as PV is shared between more houses. A 30 kW west facing PV array reduces E_{90} for a single house by approximately 245 kWh, but approximately 2195 kWh for a microgrid of 10 houses. This simple adjustment in how the array is used significantly improves the load consistency of a group of houses.

2. The application of PV vs. PV + storage

PV energy production is only available during daylight hours, but residential electrical loads in Boise, ID and elsewhere are high even after the sun sets. With battery storage, PV energy may be stored to be used after PV energy production has ended. A PV array generates the same amount of energy whether it is connected to a battery or not. The only difference is that the energy may be used at a later time. Storage allows for more flexibility with load modification, suggesting that the benefits from PV + storage are greater than the benefits from PV. The maximum $P_{p,red}$ and $E_{90,avoid}$ were calculated and used to compare the application of PV + storage with the application of PV by itself. The two applications were applied to both a single house and a 10 house microgrid.

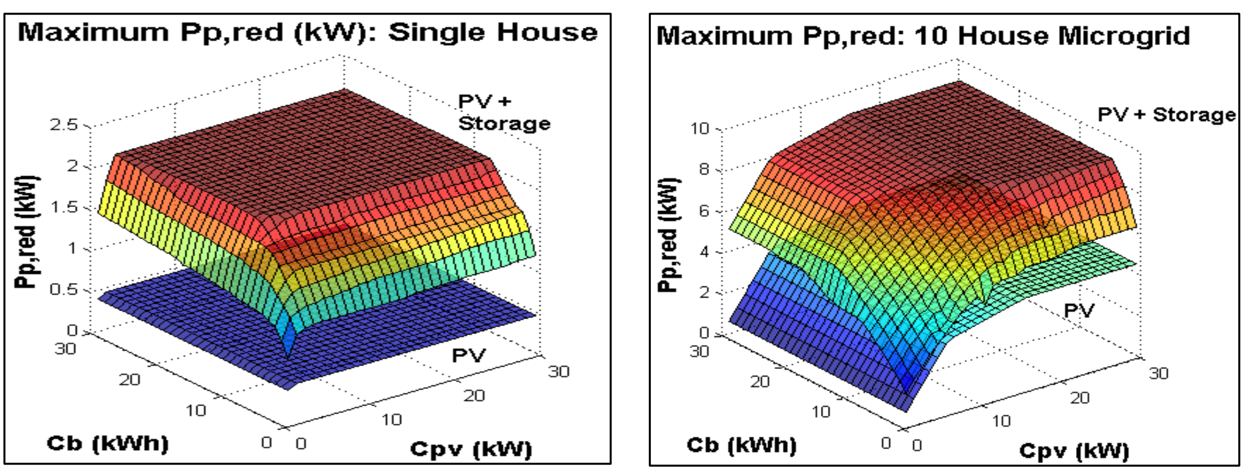

Figure 8: Maximum $P_{p,red}$ for the application of PV and PV + storage: (a) single house, (b) 10 house microgrid

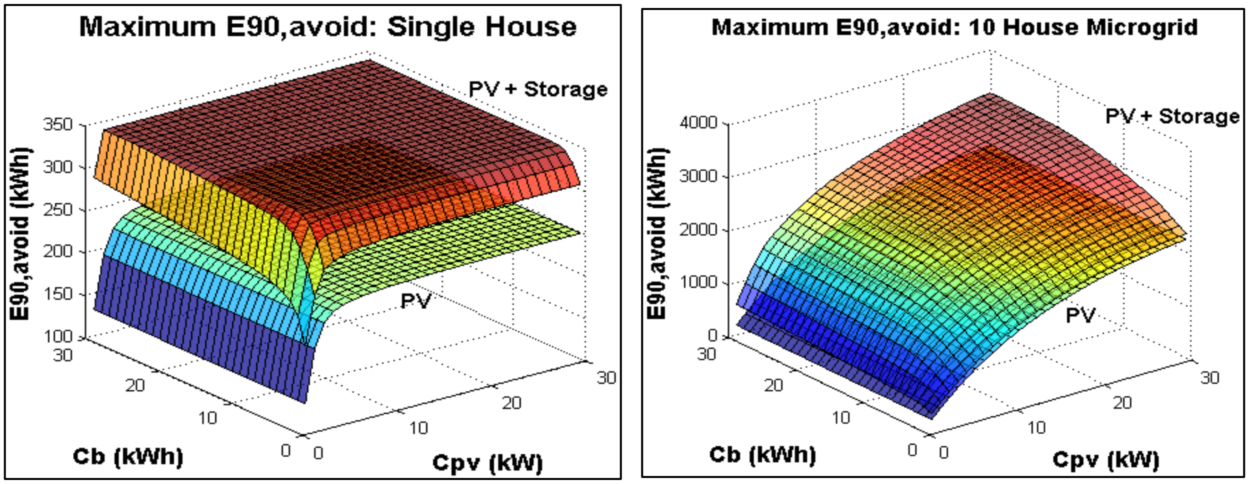

Figure 9: Maximum $E_{90,avoid}$ for the application of PV and PV + storage: (a) single house, (b) 10 house microgrid

The surfaces in Figure 8 (a) and (b) represent the maximum $P_{p,red}$ as a function of C_{pv} and C_b for the application of PV and a PV + storage. The surfaces in Figure 9 (a) and (b) represent the maximum $E_{90,avoid}$ for the same applications. A PV system has no storage capacity, which is why the PV surfaces are constant along the y-axis. The PV surfaces are projections of the intersection of the PV + storage surface with the x-z plane (C_b = 0), and can be used to visualize the benefit of adding storage capacity to a PV system.

The magnitude of the gradient ($\overrightarrow{\nabla}$) of the PV + storage surface is the approximate maximum marginal benefit of the adding an optimal amount of additional PV and storage capacity. The optimal amount of additional capacity is represented by the direction of the gradient. The marginal benefit is measured in terms of $P_{p,red}$ or $E_{90,avoid}$. In other words, the steepness of the surface is an instantaneous measure of the effectiveness of the system. At the points where $\vec{\nabla} = 0$ (the surface is flat), additional PV and storage capacity has no benefit. The same theory may be applied to the PV surface.

In Figures 8 and 9, the PV + storage surface is above the PV surface at every (x,y) position. For C_{pv}<30 and C_b<30, $P_{p,red}$ and $E_{90,avoid}$ is greater for the application of PV + storage than the application of a PV array of equivalent capacity, as long as storage is executed efficiently. When applied to a single house, PV may reduce P_p by a maximum of 0.437 kW compared to 2.070 kW from PV + storage. When applied to a 10 house microgrid, PV may reduce P_p of the aggregate load by a maximum of 4.367 kW compared to 8.867 kW from PV + storage. When applied to a single house, PV may reduce E_{90} by a maximum of approximately 246 kWh compared to 338.173 kWh from PV + storage. As shown in Figure 9 (b), there does not seem to be a limit within the range of the graph to which PV or PV + storage may reduce E_{90}. However it is clear than $E_{90,avoid}$ is greater when PV + storage is applied to a 10 house microgrid rather than PV.

3. Applying a single PV + storage system to a single home vs. a microgrid

The percentage of homeowners who have installed PV and storage systems on their houses is small, even though they are becoming increasingly popular. If the grid were made up of many microgrids each sharing a PV + storage system, the percent of homes that would have access to these resources would increase tremendously. In addition, results suggest that PV + storage systems are more beneficial when applied to a microgrid rather than a single home.

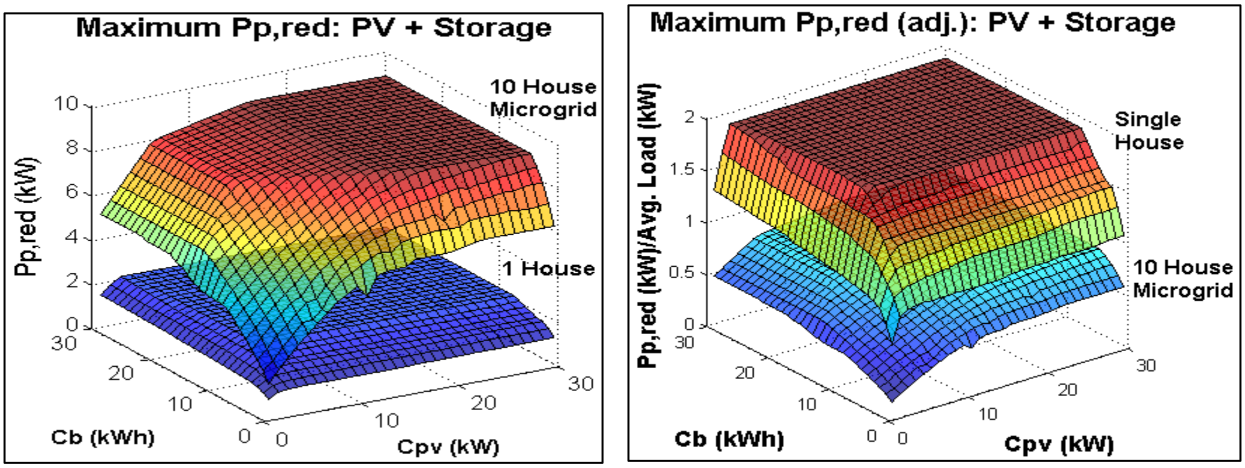

Figure 10: Maximum $P_{p,red}$ from the application of PV + storage to a single house and a microgrid: (a) not normalized for avg. load, (b) normalized for avg. load

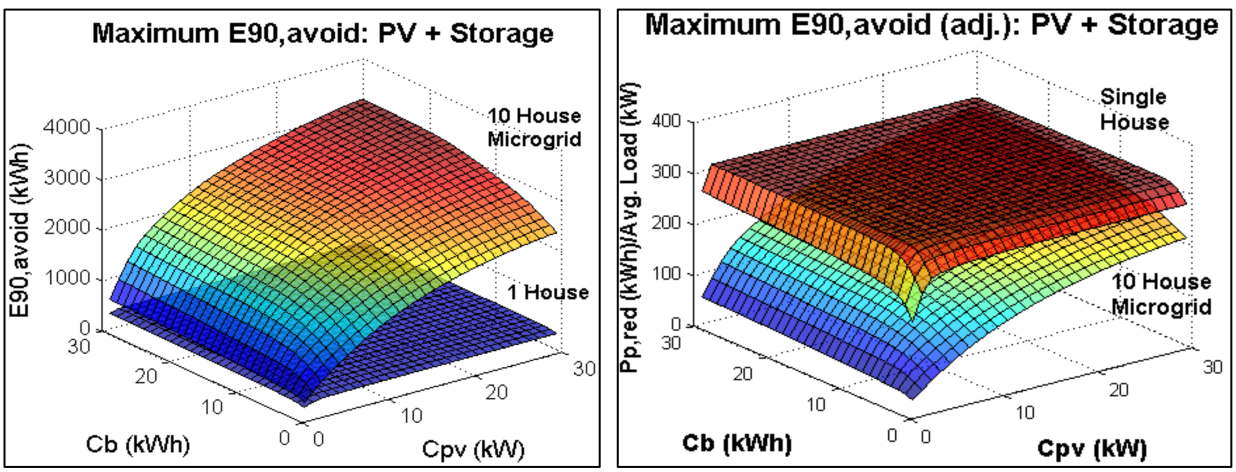

Figure 11: Maximum $E_{90,avoid}$ from the application of PV + storage to a single house and a microgrid: (a) not normalized for avg. load, (b) normalized for avg. load

Figures 10 and11 compare the effects of applying a single PV + storage system to single house and a microgrid. Figures 10 (a) and 11 (a) show the overall effect of the system on the overall load. The data is not normalized to account for the difference in the number of houses. $P_{p,red}$ and $E_{90,avoid}$ for the load of a single house and the aggregate load of a microgrid are measured despite the fact that the two loads are of different magnitudes. Figures 10 (b) and 11 (b) are normalized to account for the difference in the number of houses. The z-axes measure $P_{p,red}$/avg. load and $E_{90,avoid}$/avg. load. Since the average load of the modeled Boise house is approximately 1.105 kW, the z-axis can nearly be interpreted as $P_{p,red}$ or $E_{90,avoid}$ per home. All four graphs display the maximum attainable values of $P_{p,red}$ and $E_{90,avoid}$ when PV + storage is applied to a single house or microgrid.

In Figures 10 (a) and 11 (a), the 10 house microgrid surface is always greater than the single house surface, so the overall benefit in terms of $P_{p,red}$ and $E_{90,avoid}$ from applying a single PV + storage system to a microgrid is greater than the benefit of applying the system to a single home. However in Figures 10 (b) and 11 (b) the single house surface is always above the microgrid surface. When the same PV + storage system is applied to both a single house and a microgrid, $P_{p,red}$ for a single house is greater than $P_{p,red}$ for one of the houses in the microgrid, but the sum of $P_{p,red}$ for all of the houses in the microgrid is larger than $P_{p,red}$ for a single house. The same is true for $E_{90,avoid}$. The overall effect of the system is the most important, since a utility must meet the aggregate load of all of the houses connected to the grid, not just the ones that are sharing a PV + storage system.

As shown in Figure 11 (a), a PV + storage system can reduce E_{90} for a microgrid by more than 3100 kWh but only approximately 338 kWh for a single house. In addition, the surface for a 10 house microgrid in Figure 11 (a) never flattens out within the range of the graph while the surface for a single house flattens out with at least 9 kW PV capacity and 5 kW storage capacity. More capacity may be applied to a microgrid than a single house before the additional capacity becomes ineffective in reducing E_{90}.

4. Appropriate sizing of C_{pv} and C_b

PV and PV + storage systems seem to be only capable of reducing P_p to a certain limit regardless of C_{pv} and C_b. Once that limit is reached, additional PV and storage capacity is ineffective in reducing $P_{p.}$ Therefore, PV and storage systems must be sized to avoid installing unnecessary capacity for peak shaving.

The four surfaces in Figure 10 represent $P_{p,red}$ for four different applications: PV and PV + storage applied to both a single house and a microgrid. Each line plot in Figure 12 is the projection onto the x-y plane of the section of a surface where $\vec{\nabla} = 0$. The area left and below each line represents the combinations of C_{pv} and C_b that are effective in reducing P_p. Increases in C_{pv} or C_b over the line do not reduce P_p. All of the points on each line represent efficient capacity combinations that maximize $P_{p,red.}$ The most economic point on the line is likely along the section nearest the origin, and could be determined by comparing the unit cost of storage and PV capacity.

As shown in Figure 12, the C_{pv} limit for effective P_p reduction increases significantly as the number of houses sharing PV + storage increases, but the C_b limit decreases by a minimal amount. To minimize P_p, it appears that a 10 house microgrid requires significantly more PV capacity and a similar amount of storage capacity compared to a single house.

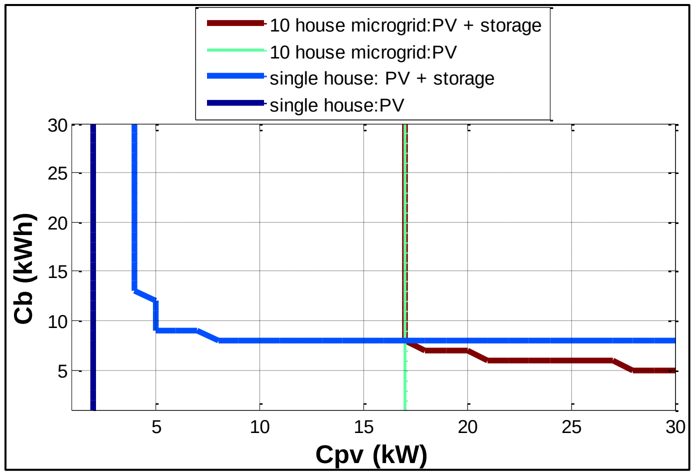

Figure 12: Contour plot of $P_{p,red}$ data at maximum $P_{p,red}$ values

5. Economic Modeling Results

Table 2 gives the estimated cost of purchased power per year for each of the four modeled scenarios based on the residential rate charged to each house individually, the residential rate charged assuming that the houses were aggregated behind a single point of common connection (PCC), and the LGS rate assuming aggregation behind a single PCC. The fixed customer service charge was subtracted from each schedule under the assumption that service costs for each scenario would not vary to any meaningful extent and to allow for a comparison based solely on demand and energy charges. It was also assumed that aggregating multiple homes behind a single PCC would qualify the microgrid for listing under the LGS rate schedule.

Table 2: Estimated cost of power purchases

Scenario	Standard Residential	Aggregated Standard Residential	Large General Service
Base Case	$7,957	$9,724	$6,072
5 x 5	$7,493	$9,126	$5,625
10 x 10	$7,029	$8,530	$5,296
20 x 20	$6,102	$7,337	$4,672

The residential rate case is compared to the LGS case in order to contrast the estimated cost of purchased power between a case based solely on energy charges (residential) with a case that incorporates both energy and demand charges (large general). The point of comparing the two types of schedules was to investigate the impact of preferentially decreasing peak power demand over energy demand. As can be seen in Table 2, the LGS plan provides for the lowest annual cost of purchased power followed by the standard residential rate applied individually to each home. The higher costs of the aggregated residential rate case can be primarily attributed to reaching higher pricing tiers earlier in the billing period. To be equitable, such an arrangement would require a modification of the pricing tiers to account for demand aggregation. A comparison of the cost savings for each rate case between scenarios is presented in Table 3. The values presented in Table 3 show that there is minimal difference in costs savings between schedules on a percentage basis with increasing penetration of PV generation and battery storage. The annual cost of purchased power decreases linearly under all three rate cases.

Table 3: Comparison of savings on purchases power

Scenario	Standard Residential		Aggregated Standard Residential		Large General Service	
	$ Delta	% Delta	$ Delta	% Delta	$ Delta	% Delta
5 x 5	464	5.8	598	6.1	447	7.3
10 x 10	928	11.7	1194	12.2	776	12.8
20 x 20	1855	23.3	2387	24.5	1400	23.1

Table 3 gives the reduction in cost for E90 energy purchases that results from the decrease in the P90 power demand for each of the four scenarios. The E90 savings estimate was made from the utility's perspective using Idaho Power's published threshold rate for the cost of demand side management (DSM) programs (Idaho Power, 2013) and is independent of a given rate structure. The cost of demand side management is used instead of the cost of additional generation because of the assumption that the microgrid does not provide power or services to the bulk grid. This assumption means that from the utility standpoint the microgrid more closely resembles an energy efficiency measure rather than a generation or grid services application. The goal of making the estimate presented in Table 6.3 is to attempt make an initial quantification of the value to the utility of using the microgrid as a demand side management application to preferentially decrease peak consumption.

Table 4: Reduction in the cost of E90 purchases

Scenario (E90)	$ Delta	% Delta
5 x 5	173	13.1
10 x 10	317	24.0
20 x 20	562	42.6

Table 4 shows that the decrease in the cost of E90 energy is greater in percentage terms that the overall rate of decrease given in Table 1 due to a reduction in the amount of higher cost peak power. However, the rate of decrease in costs could be expected to reach a limit as peak power purchases are increasingly eliminated. Tables 2,3 and 4 provide some confirmation that a community microgrid employing PV and battery storage has the potential to provide cost savings to both a utility and to consumers. However, it should be stressed that the values given in the tables are very rough top-down estimates made using adaptations of utility rates that have not been tailored to handle the scenarios modeled in this paper. A more refined cost-benefit study based on a detailed analysis of local conditions at a given distribution feeder would be required to produce bankable information suitable for deployment. This analysis also does present an estimate of the net present value of the modeled systems, an evaluation of the additional benefits of a microgrid, or a comparison to costs and benefits of alternative methods and technologies.

Future Work

This paper presents the development of a modeling framework to investigate the technical and economic merits of distributed generation and storage in context of microgrids. The preliminary results show that the aggregation made possible by microgrids allows us to capture the non-energy benefits of distributed energy technology. The framework also opens up the possibility of optimal sizing of resources for maximum technical and economic benefit.

This work is continuing along three related lines. First, we are developing a Demand Response model that will allow us to tie demand response events (through thermostat set points) to conditions at the individual homes (as opposed to centrally dispatched DR). The goal is to further leverage the generation and storage to reduce peak loads and energy even greater. It is expected that we will see similar synergistic behavior in that a modest amount of demand response may yield much better returns in non-energy benefits.

Second, we are developing the model of the microgrid to incorporate variability of the individual homes. By utilizing public domain data [11] we hope to mimic the randomness of actual homes as well as the variability of peak hours of operation. This will be essential to developing realistic DR programs.

Finally, we are looking at model predictive control of small commercial buildings with radiant slab heating and cooling. We hope to incorporate an energy storage aspect to the control scheme which will allow us to add an important resource to our microgrid model.

References

[1] Garcia, H.E., A. Mohanty, W-C Lin, R. Cherry. 2013. “Dynamic analysis of hybrid energy systems under flexible operation and variable generation”, *Energy*. **52**:1, pp 1-32.
[2] Baylon, D., Storm, P., Geraghty, K., Davis, B. 2012. “2011 Residential Building Stock Assessment: Single-Family Characteristics and Energy Use.” Northwest Energy Efficiency Alliance.
[3] U.S Energy Information Administration. 2009. “2009 RECS Survey Data. Housing Characteristics.”
[4] Wilson, E., Engebrecht Metzger, C., Horowitz, S., Hendron, R. 2014. “2014 Building America House Simulation Protocols.” National Renewable Energy Laboratory.
[5] Leadbetter, J., Swan, L. 2012. “Battery storage system for residential electricity peak demand shaving.” *Energy and Buildings* 55: 685-692.
[6] 2014. “Documentation Center MATLAB.” MathWorks.
[7] Mondol, J. D., Yohanis, Y. G., Norton, B. 2007. “The impact of array inclination and orientation on the perforamance of a grid-connected photovoltaic system.” *Renewable Energy* 32: 118-140
[8] Idaho Public Utilities Commission, "Approved Electric Tariffs," 2014. [Online]. Available: http://www.puc.idaho.gov/fileroom/tariff/electric/approved.html. [Accessed 20 August 2014].

[9] Blank, L., Gegax, D. (2014). Residential Winners and Losers behind the Energy versus Customer Charge Debate. *The Electricity Journal,* 27 (4), 31-39.
[10] Idaho Power Co., "2013 Integrated Resource Plan," Idaho Power, Boise, 2013.
[11] Pecan Street Research Institute. 2013. “Report: Residential Solar Systems Reduce Summer Peak Demand by Over 50% in Texas research trial.”